Asian Journal of Andrology (2021) 23, 231–235
www.asiaandro.com; www.ajandrology.com

Open Access

ORIGINAL ARTICLE

Prostate Disease

Developing a coordinate-based strategy to support cognitive targeted prostate biopsies and correlative spatial-histopathological outcome analysis

Keiran D Clement[1], Lizzy Day[2], Helen Rooney[1], Matt Neilson[3], Fiona Birrell[1], Mark Salji[1,3,4], Elizabeth Norman[1], Ross Clark[2], Amit Patel[5], John Morrison[5], Hing Y Leung[1,3,4]

Lack of investment for magnetic resonance (MR) fusion systems is an obstacle to deliver targeted prostate biopsies within the prostate cancer diagnostic pathway. We developed a coordinate-based method to support cognitive targeted prostate biopsies and then performed an audit on cancer detection and the location of lesions. In each patient, the prostate is considered as two separate hemiprostates, and each hemiprostate is divided into 4 × 4 × 4 units. Each unit is therefore defined by a three-dimensional coordinate. We prospectively applied our coordinates approach to target 106 prostatic lesions in 93 men. Among 45 (of 106; 42.5%) lesions positive for cancer, 27 lesions (60.0%) harbored clinically significant disease. PSA density was significantly higher in patients with proven cancer (median: 0.264 ng ml^{-2}) when compared to the noncancer group (median: 0.145 ng ml^{-2}; $P = 0.003$, Wilcoxon rank-sum test). Lesions with Prostate Imaging-Reporting and Data System (PIRADS) score of 5 were found to have a cancer incidence of 65.2%, while PIRADS 4 and 3 lesions have a lower risk of cancer detection, as expected, at 37.3% and 31.3%, respectively. The probability of a lesion being cancerous in our series significantly decreases as we go from the "apex-to-base" dimension (odds ratio [OR]: 2.62, 95% confidence interval [CI]: 1.55–4.44, $P = 0.00034$). Our analysis also indicates that the probability of cancer decreases as the prostate volume increases (OR: 1.03, 95% CI: 1.01–1.05, $P = 0.00327$). Based on this feasibility study, the use of coordinates to guide cognitive targeted prostate biopsies warrants future validation study in additional centers.

Asian Journal of Andrology (2021) **23**, 231–235; doi: 10.4103/aja.aja_49_20; published online: 24 November 2020

Keywords: cognitive targeted prostate biopsies; coordinates; magnetic resonance imaging; prostate cancer

INTRODUCTION

Prostate cancer is the second most common malignancy affecting men worldwide.[1] Opportunistic screening for prostate cancer with prostate-specific antigen (PSA) testing and digital rectal examination may result in unnecessary prostate biopsies and the detection of indolent disease, resulting in risk of overtreatment particularly in clinically insignificant prostate cancer. Prebiopsy multiparametric magnetic resonance imaging (mpMRI) of the prostate is significantly impacting on the diagnostic pathway of prostate cancer.[2,3] For the majority of centers with a targeted prostate biopsy service, both MRI-transrectal ultrasound (MRI-TRUS) fusion biopsies and cognitive targeted biopsies are deemed acceptable, with similar cancer detection incidence in a recent systematic review.[4,5]

MRI-guided in-bore prostate biopsies are reported to be the most accurate, but suffer from high (setup and running) costs, with one recent study finding an increase in costs of 150% for fusion biopsy with sedation and 125% for in-bore MRI biopsy with sedation compared to standard TRUS-biopsy.[6] Furthermore, in-bore MRI biopsy has a low throughput and requires substantial technical requirements and results in significant discomfort to patients.[7–9]

Cognitive targeted biopsies require the least amount of financial investment, but its success depends on a high level of technical expertise in both MRI interpretation and real time localization of the target lesion(s).[10] The relationship between lesion characteristics (such as size and localization) and cancer detection is difficult to assess.[2]

We developed a coordinate-based system to register the spatial location of prostatic lesion(s), see **Figure 1**, as a tool to support cognitive targeted prostate biopsies for patients with MRI prostate-detected lesions. In this feasibility study, we prospectively applied three-dimensional coordinates to guide cognitive targeted prostatic biopsies.

PATIENTS AND METHODS

Patient cohort for targeted prostate biopsies

Consecutive patients undergoing diagnostic investigation for prostate cancer in the Department of Urology, NHS Greater Glasgow and Clyde (South Sector), Glasgow, UK, were considered for coordinate-guided targeted prostate biopsies. Suitable patients were identified following diagnostic MRI (see details below). MR prostate imaging was performed in accordance with recent consensus recommendations.[11] Patients with detected lesions of Prostate Imaging-Reporting and Data System

[1]Department of Urology, Queen Elizabeth University Hospital, 1345 Govan Rd, Glasgow G51 4TF, UK; [2]Department of Urology, Ayr University Hospital, Dalmellington Rd, Ayr KA6 6DX, UK; [3]CRUK Beatson Institute for Cancer Research, Garscube Estate, Bearsden, Glasgow G61 1BD, UK; [4]Institute of Cancer Sciences, University of Glasgow, Bearsden, Glasgow G61 1BD, UK; [5]Department of Radiology, NHS Greater Glasgow and Clyde, Glasgow G51 4TF, UK.
Correspondence: Dr. HY Leung (h.leung@beatson.gla.ac.uk)
Received: 20 January 2020; Accepted: 28 June 2020

(PIRADS) v2 score 3 or above were included in this study. Patients were excluded if they had (1) PIRADS v2 score 1 or 2 lesions (which are associated with significantly reduced likelihood of yielding clinically significant prostate cancer[12]), (2) previous history of a diagnosis of prostate cancer, including those patients on active surveillance, or (3) extensive lesions within the prostate visualized by MRI as these lesions are expected to be detected by standard (transrectal ultrasound, TRUS, guided) peripheral zone sampling biopsies. Ninety-three men (July 2017–May 2018) with 106 targetable lesions were identified and received targeted (transrectal) biopsies as part of their diagnostic investigations. Auditing of the data was performed in accordance with the local policy of the Audits Department, NHS Greater Glasgow and Clyde Health Board. Patient consent was not required as cognitive targeted prostate biopsies are part of routine clinical practice. To ensure consistency, coordinates from consecutive cases deemed suitable for targeted biopsies (namely PIRADS 3 or above) were determined by a single radiologist and prostate biopsies (n = 2–3 per lesion) were then performed by a single urologist. Systematic biopsies of the prostate were not undertaken at the time of targeted biopsies, with only the lesions of interest being sampled. In patients with more than one targetable lesion of PIRADS ≥3, these were biopsied in turn during the same sitting, with individual coordinates obtained for each lesion of interest. All patients were biopsied transrectally. No patients were on an active surveillance protocol for known prostate cancer. Clinically significant disease in this patient cohort is defined as Gleason score ≥7 or Gleason 6 with PSA >20 ng ml^{-1}.

Diagnostic MRI prostate scan

Selected MRI scanners within NHS Greater Glasgow and Clyde were optimized for MR prostate imaging. 1.5 Tesla field strength MRI scanners (Siemens Aera scanners, Siemens, Germany; Philips Ingenia, Philips, Eindhoven, the Netherlands) were used with a body array coil to image the prostate and pelvis. Sequences obtained included small field of view (FOV) multiplanar T2-weighted imaging (sagittal, axial, and coronal planes, 3-mm thickness) and axial diffusion-weighted imaging (DWI), with dynamic contrast-enhanced (DCE) imaging in selected patients. DWI b-values varied by scanner model but invariably included high b-values of up to 1400 s mm^{-2}. The b-values and apparent diffusion coefficient (ADC) mapping were assessed qualitatively.

Three-dimensional coordinate system for registering lesions of interest

For each hemiprostate, each dimension is split into four equally sized intervals, which are numbered 1–4. As illustrated in **Figure 1**, the X-coordinate denotes the relative distance from the midline (urethra) to the lateral margin of the prostate, in a right or left orientation. Similarly, the Y- and Z-coordinates denote the relative distance from the apex to the base and from the rectum forward (toward the pubic symphysis) of the prostate gland, respectively. Using this coordinate system, we can then assign one or more coordinate tuples to each lesion depending on its location and size. In **Figure 1**, the XZ (or transverse) view of the prostate corresponds to the transverse image during TRUS of the prostate, while the YZ (or sagittal) view mirrors that seen for the longitudinal view of the prostate during TRUS imaging. At the time of performing cognitive (transrectal) targeted prostate biopsies, the practitioner rotates the TRUS probe to the required X (medial-to-lateral) coordinate while maintaining alignment to the prostate; following which, angulation of the TRUS probe then allows the targeting of specific location in accordance of the Y and Z coordinates as assessed by the sagittal (YZ) view.

Statistical analyses

To examine the relationship between the location of lesions and their respective histopathology outcome, we fit a binary logistic regression

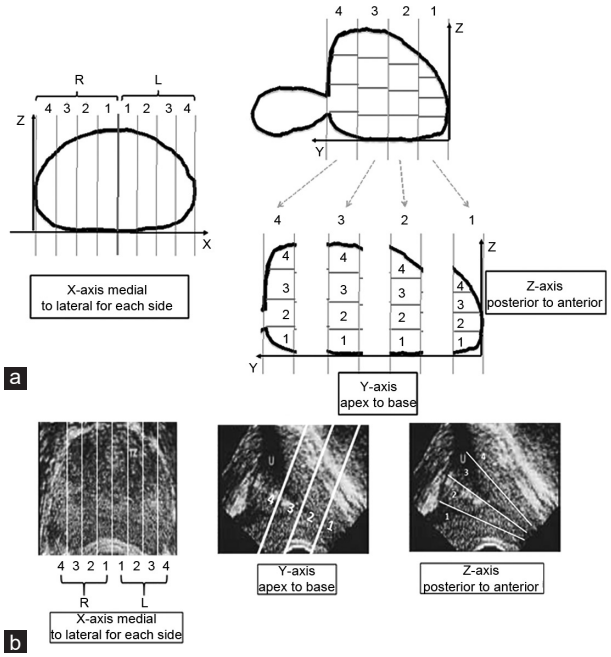

Figure 1: Cross-sectional view of the three-dimensional coordinate system that is used to target lesions of interest. (**a**) Cartoon illustrates the coordinate system. (**b**) Images from transrectal ultrasound scan to highlight the coordinates in each of the three axes. The X-axis is oriented laterally, with +1 to +4 denoting lesions on the right-hand-side of the midline and −1 to −4 denoting lesions on the left-hand-side of the midline. The Y-axis is oriented longitudinally, with 1 denoting the apex of the gland and 4 denoting the base of the gland. The Z-axis is oriented such that 1 denotes the posterior region of the gland and 4 denotes the anterior region of the gland. Note that the scale of each axis varies depending on the size of the prostate. R: right; L: left.

model within a Generalized Estimating Equations[13] framework to the data. Generalized Estimating Equations allow the estimation of parameters of a generalized linear model with the potential for a possible unknown correlation between outcomes (in this case lesion location and histopathological outcome). The three coordinate values (X, Y, and Z) and prostate volume were included as independent variables, subject was included as the cluster identifier, and cancer status (histopathological outcome: cancer versus benign) was taken to be the response variable. Full details of the methodology are included in the **Supplementary Information**.

RESULTS

Coordinates from consecutive cases deemed suitable for targeted biopsies (lesions with PIRADS ≥3) were determined and prostate biopsies were performed, with 2–3 tissue cores obtained per lesion. Ninety-three men (July 2017–May 2018) with 106 targetable lesions were studied. **Table 1** shows the patient demographics and relevant clinical parameters. Consistent with reported series of targeted prostate biopsies,[14,15] Forty-two of 93 (45.2%) patients were found to have prostate cancer, with 25 (59.5%) of 42 men affected by clinically significant disease (**Table 2** and **3**). Looking at individual lesions, among 45 of 106 lesions (42.5%) positive for cancer, 27 lesions (60.0%) harbored clinically significant disease (defined as Gleason score ≥7 or Gleason 6 with PSA >20 ng ml^{-1}). PSA density was significantly higher in patients with proven cancer (median: 0.264 ng ml^{-2}, interquartile range [IQR]: 0.240) when compared to the noncancer group (median: 0.145 ng ml^{-2}, IQR: 0.116; P = 0.003, Wilcoxon rank-sum test; **Figure 2**). Lesions with PIRADS score of 5 were found to have a

Table 1: Patient demographic and clinicopathological information

Patient factors	*All*	*Benign*	*Insignificant cancer*	*Significant cancer*
Age (year), mean (median, range)	66.91 (67, 42–80)	65.50 (65.5, 42–80)	65.72 (66, 56–77)	70.89 (72, 46–79)
PSA (ng ml^{-1}), mean (median, range)	11.00 (8.90, 0.2–52.6)	9.37 (8.00, 0.2–31.2)	8.60 (7.85, 4.4–19.6)	15.63 (14.95, 1.7–52.6)
Prostate volume (cm^3), mean (median, range)	51.17 (43.40, 17.2–142.0)	56.57 (54.20, 17.2–142.0)	47.57 (39.40, 24.5–104.0)	38.87 (33.00, 19.1–79.4)
Number of previous biopsies (*n*), mean (median, range)	0.96 (1, 0–4)	0.98 (1, 0-4)	0.72 (1, 0–3)	1.00 (1, 0–3)

Mean values shown with median and range in bracket. See **Supplementary Information** on statistical analysis on association between individual parameters and cancer status. PSA: prostate-specific antigen

Table 2: The breakdown of histopathology outcome according to the reported Prostate Imaging-Reporting and Data System scores

PIRADS/histology	*Benign*	*Overall cancer*	*Clinically insignificant cancer*	*Clinically significant cancer*	*Atypia*
3, *n* (%)	10 (62.5)	5 (31.3)	5 (31.3)	0 (0)	1 (6.3)
4, *n* (%)	41 (61.2)	25 (37.3)	7 (10.4)	18 (26.9)	1 (1.5)
5, *n* (%)	7 (30.4)	15 (65.2)	6 (26.1)	9 (39.1)	1 (4.3)

Total number of lesions=106. PIRADS: Prostate Imaging-Reporting and Data System

Table 3: The breakdown of prostate cancer (*n*=45) identified by coordinates guided cognitive targeted prostate biopsies

Gleason grade (Group 1–5)	*Number of lesion (n)*	*Number of patient (n)*
1	21	20
2	18	17
3	3	3
4	3	3
5	0	0

Three patients with Gleason Grade 1 disease presented with PSA >20 ng ml^{-1} were included in the significant cancer group for analysis. PSA: prostate-specific antigen

cancer incidence of 65.2%, while PIRADS 4 and 3 lesions have a lower risk of cancer detection, as expected, at 37.3% and 31.3%, respectively.

We performed spatial outcome analysis based on the coordinates of individual lesions and the respective "cancer versus noncancer" status following prostate biopsies. From the data on incidence and histopathology outcome in the XY, XZ, and YZ marginal planes (**Figure 3**, **Supplementary Figure 1** and **Supplementary Information**), we observed a possible trend along the Y dimension (from prostatic apex to base), with lower Y values (nearer the apex of the prostate) associated with a relatively higher proportion of cancerous lesions. From our binary logistic regression model (with Generalized Estimating Equations), the *P*-values for the X, Y, Z, and prostate volume coefficients were 0.2751, 0.0003, 0.0903, and 0.0033, respectively (**Supplementary Table 1**), suggesting a potential association between the Y component and prostate volume with the detection of cancer following targeted biopsies. Specifically, we found that for every unit increase in Y (*i.e.*, as we tend toward the prostatic base), the odds of cancer detection decreases by a factor of 2.62 (95% confidence interval [CI]: 1.55–4.44). The drop in cancer detection toward the prostatic base can arise from inadequate number of biopsy cores taken and/or technical deficiency. Our analysis also revealed an association between prostate volume and the detection of cancer; with the model indicating that for every 1 ml increase in prostate volume, the odds of cancer detection decreases by a factor of 1.03 (95% CI: 1.01–1.05).

DISCUSSION

Template or sector-based approaches such as the Ginsberg protocol[16] can direct biopsies to the individual prostatic "zones." For cognitive targeted biopsies, urologists interpret the scans themselves or collaborate with uroradiologists to mark up lesion(s) on paper-based

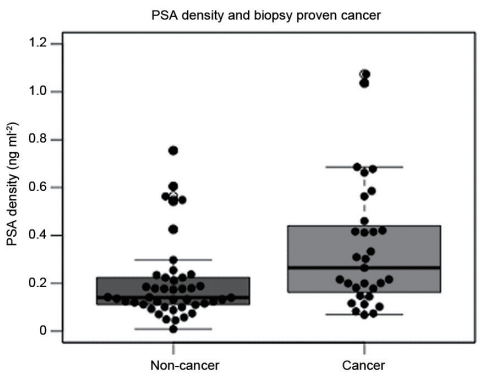

Figure 2: Box and Whisker plot summarizing the analysis of PSA density between cancer and noncancer groups. PSA density is significantly greater in patients with targeted biopsy proven cancer (median: 0.264 ng ml^{-2}, IQR: 0.240), when compared to noncancer group (median: 0.140 ng ml^{-2}, IQR: 0.116; $P = 0.003$, Wilcoxon rank-sum test). In the Box and Whisker diagram, the middle band represents the median value, the upper and lower box represents the upper and lower quartiles, whiskers extend from the upper and lower quartiles by 1.5× the interquartile range, individual patients are also plotted as solid black points overlaid on the boxplots. PSA: prostate-specific antigen; IQR: interquartile range.

templates, with predetermined prostatic zones, *e.g.*, 12 segments, namely left and right; basal, mid, and apical; and anterior or posterior[17] or as many as 24 regions as described by Haffner *et al.*[18] However, urologists will need to refer to the hand-drawn template map during the biopsy procedure, and radiologists will need to spend time to mark up the template maps in multiple planes. The coordinate approach avoids the need for the radiologists to physically draw on a template map and can direct prostate biopsies via both transrectal and transperineal routes with minimal setup time. This report is based on a single urologist/uroradiology partnership. It is necessary to carry out validation in other centers.

The value of input from uroradiologists is well reported and is associated with enhanced cancer detection rates. A cancer detection rate of 33.1% (131/396) was reported when cognitive biopsies were performed by a urologist alone.[19] Higher cancer detection rates of 68.5% (37/54), or 48.6% for clinically significant disease, can be achieved when a uroradiologist was present during biopsies.[11] The coordinate approach only requires the uroradiologist to nominate the location of the target lesion(s) in the predetermined X-Y-Z axes rather than

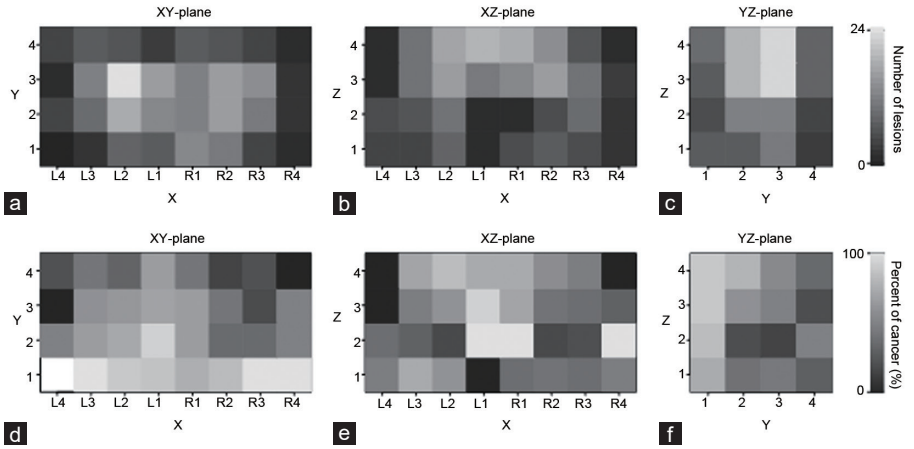

Figure 3: Marginal distribution of lesions for the (**a**) XY plane, (**b**) XZ plane, and (**c**) YZ plane, where we see that the more lesions cover the central area of the X and Y axes, and the higher area of the Z-axis. We also include marginal distributions for the proportion of lesions that are cancerous in the (**d**) XY plane, (**e**) XZ plane, and (**f**) YZ plane. Note that there appears to be a possible trend along the Y-axis, with lower values of Y possibly corresponding to a higher proportion of cancerous lesions. X: midline to lateral for right and left of the prostate; Y: apex to base of the prostate; Z: posterior to anterior of the prostate. Therefore, XY plane signifies the transverse plane, XZ plane refers to coronal (frontal) plane, and YZ plane represents sagittal. R: right; L: left.

physically marking up the lesion in each plane; this process is quicker, reducing the reporting time.

We have constructed a three-dimensional coordinate-based system for targeting prostate lesions. Our exploratory analysis revealed a possible association between the Y-coordinate (longitudinal axis, from the prostatic apex to the base) and histopathology. We then used binary logistic regression within a Generalized Estimating Equations framework to show that there is evidence of a relationship between the Y-coordinate of a lesion's centroid and the probability that the lesion is cancerous, where the probability of cancer decreases as the Y-coordinate increases (*i.e.*, as we move from the base to the apex of the prostate). Besides specific spatial location within the prostate, we also identified prostatic volume as a significant factor in the detection of cancer. As the absolute dimension of each coordinate unit depends on the prostate volume, additional biopsies from individual "grid" units may be required in larger prostates, as described previously.[20] The use of Generalized Estimating Equations supports the analysis of all lesions from our patient cohort regardless of the number of lesion(s) present in individual patients, thus avoiding the need to assume individual lesions within the same patient being independent or to average the information from the coordinates of different lesions within one prostate gland.

Irrespective of the registration method utilized, MRI-targeted prostate biopsies outperform systematic biopsies for the detection of clinically significant cancer.[2] However, MRI-guided fusion biopsy of the prostate does come at significant cost, with fusion biopsy approach estimated to be 2.5 times more expensive than standard TRUS-guided systematic (sampling) biopsy of the prostate.[6] Cognitive biopsy of the prostate is less expensive than fusion biopsy as it is quicker and nullifies the need for a fusion-platform device as well as the time for fusion registration of the images to an ultrasound machine.[21] Furthermore, in a randomized controlled trial comparing systematic biopsy versus systematic biopsy plus MRI-guided cognitive targeted biopsy of the prostate, mpMRI-guided cognitive biopsy of the prostate significantly improved the detection of clinically significant prostate cancer.[22] Compared to the literature on "learning curve" associated with targeted prostate biopsy by fusion-targeted prostate biopsy,[23–25] to our knowledge, the evidence outlining the learning curve and risk of operator-related targeting errors for cognitive biopsy of the prostate is lacking, with only one reported small single-surgeon series evaluating the learning curve which proposed the need for further studies.[26] We developed and piloted a coordinate-based approach to support cognitive targeted prostate biopsies, demonstrating comparable clinically significant cancer detection rates to other published series.[27] Our hope is that our coordinate-based approach may reduce the "variability" of targeting lesions during cognitive prostate biopsy and "flatten" the learning curve.

Our study is based on a single surgeon-radiologist series to test the feasibility of the coordinates system to support cognitive targeted prostate biopsies. Some of the patients had had previous negative systematic TRUS-guided biopsies of the prostate, but none of our cohort were on an active surveillance program for known prostate cancer. Our results may therefore not be generalizable to all patient subgroups. We believe that the coordinates system can be easily applied in a transperineal route of biopsy. A future study to evaluate the application of the coordinates in transperineal-based biopsies is required as transperineal prostate biopsies are increasingly adopted to minimize the risk of biopsy-related sepsis.[28] In our series, three of 93 patients experienced significant adverse symptoms that warranted hospital admission within 30 days of targeted prostate biopsies. Three patients (3.2%) developed urinary sepsis. No patients (0%) experienced urinary retention. While we may expect a lower risk of sepsis with targeted biopsies as fewer biopsies were performed on each patient, the absolute risk of an infective episode among our patients may be increased as many of them have had previous prostate biopsies, with 61 of 93 (66.0%) had one or more sets of transrectal prostatic biopsies before.

Collectively, our data suggest that the coordinate-based approach is a simple tool to support targeted prostate biopsies. The coordinate-based approach can be applied for both transrectal and transperineal prostate biopsies. Ultimately, these data need to be correlated to data from pathologic evaluation in those patients undergoing radical prostatectomy. It will be useful to carry out external validation on the reproducibility of the coordinate system in other centers. We propose that the use of coordinates will facilitate the adoption of prebiopsy MR of the prostate without capital investment and staff costs associated with MRI-TRUS fusion systems.

AUTHOR CONTRIBUTIONS

JM and HYL designed the study; KDC, LD, HR, FB, MS, EN, RC, AP, JM, and HYL conducted and collected data; KDC, MN, MS, and HYL analyzed data and made interpretations; and KDC, LD, and HYL wrote the manuscript. All authors read and approved the final manuscript.

COMPETING INTERESTS

All authors declared no competing interests.

ACKNOWLEDGMENTS

Research in the Leung Laboratory at the Beatson Institute is supported by Cancer Research UK (C596/A17196, CRUK A15151).

Supplementary Information is linked to the online version of the paper on the *Asian Journal of Andrology* website.

REFERENCES

1 Ferlay J, Soerjomataram I, Dikshit R, Eser S, Mathers C, *et al*. Cancer incidence and mortality worldwide: sources, methods and major patterns in GLOBOCAN 2012. *Int J Cancer* 2015; 136: E359–86.
2 Kasivisvanathan V, Stabile A, Neves JB, Giganti F, Valerio M, *et al*. Magnetic resonance imaging-targeted biopsy versus systematic biopsy in the detection of prostate cancer: a systematic review and meta-analysis. *Eur Urol* 2019; 76: 284–303.
3 Ahmed HU, El-Shater Bosaily A, Brown LC, Gabe R, Kaplan R, *et al*. Diagnostic accuracy of multi-parametric MRI and TRUS biopsy in prostate cancer (PROMIS): a paired validating confirmatory study. *Lancet* 2017; 389: 815–22.
4 Wegelin O, van Melick HH, Hooft L, Ruud Bosch JL, Reitsma HB, *et al*. Comparing three different techniques for magnetic resonance imaging-targeted prostate biopsies: a systematic review of in-bore versus magnetic resonance imaging-transrectal ultrasound fusion versus cognitive registration. Is there a preferred technique? *Eur Urol* 2017; 71: 517–31.
5 Giganti F, Moore CM. A critical comparison of techniques for MRI-targeted biopsy of the prostate. *Transl Androl Urol* 2017; 6: 432–43.
6 Altok M, Kim B, Patel BB, Shih YC, Ward JF, *et al*. Cost and efficacy comparison of five prostate biopsy modalities: a platform for integrating cost into novel-platform comparative research. *Prostate Cancer Prostatic Dis* 2018; 21: 524–32.
7 Venderink W, van Luijtelaar A, Bomers JG, van der Leest M, Hulsbergen-van de Kaa C, *et al*. Results of targeted biopsy in men with magnetic resonance imaging lesions classified equivocal, or highly likely to be clinically significant prostate cancer. *Eur Urol* 2018; 73: 353–60.
8 Pokorny MR, de Rooij M, Duncan E, Schröder FH, Parkinson R, *et al*. Prospective study of diagnostic accuracy comparing prostate cancer detection by transrectal ultrasound-guided biopsy versus magnetic resonance (MR) imaging with subsequent MR-guided biopsy in men without previous prostate biopsies. *Eur Urol* 2014; 66: 22–9.
9 Overduin CG, Fütterer JJ, Barentsz JO. MRI-guided biopsy for prostate cancer detection: a systematic review of current clinical results. *Curr Urol Rep* 2013; 14: 209–13.
10 Verma S, Choyke PL, Eberhardt SC, Oto A, Tempany CM, *et al*. The current state of MR imaging–targeted biopsy techniques for detection of prostate cancer. *Radiology* 2017; 285: 343–56.
11 Appayya MB, Adshead J, Ahmed HU, Allen C, Bainbridge A, *et al*. National implementation of multi-parametric magnetic resonance imaging for prostate cancer detection – recommendations from a UK consensus meeting. *BJU Int* 2018; 122: 13–25.
12 Sathianathen NJ, Knety BR, Soubra A, Metzger GJ, Spilseth B, *et al*. Which scores need a core? An evaluation of MR-targeted biopsy yield by PIRADS score across different biopsy indications. *Prostate Cancer Prostatic Dis* 2018; 21: 573–8.
13 Hubbard AE, Ahern J, Fleischer NL, Van der Laan M, Lippman SA, *et al*. To GEE or not to GEE: comparing population average and mixed models for estimating the associations between neighborhood risk factors and health. *Epidemiology* 2010; 21: 467–74.
14 Delongchamps NB, Peyromaure M, Schull A, Beuvon F, Bouazza N, *et al*. Prebiopsy magnetic resonance imaging and prostate cancer detection: comparison of random and targeted biopsies. *J Urol* 2013; 189: 493–9.
15 Puech P, Rouviere O, Renard-Penna R, Villers A, Devos P, *et al*. Prostate cancer diagnosis: multiparametric MR-targeted biopsy with cognitive and transrectal US-MR fusion guidance versus systematic biopsy – prospective multicenter study. *Radiology* 2013; 268: 461–9.
16 Kuru TH, Wadhwa K, Chang RT, Echeveria LM, Roethke M, *et al*. Definitions of terms, processes and a minimum dataset for transperineal prostate biopsies: a standardization approach of the Ginsburg Study Group for Enhanced Prostate Diagnostics. *BJU Int* 2013; 112: 568–77.
17 Otti VC, Miller C, Powell RJ, Thomas RM, McGrath JS. The diagnostic accuracy of multiparametric magnetic resonance imaging before biopsy in the detection of prostate cancer. *BJU Int* 2019; 123: 82–90.
18 Haffner J, Lemaitre L, Puech P, Haber GP, Leroy X, *et al*. Role of magnetic resonance imaging before initial biopsy: comparison of magnetic resonance imaging-targeted and systematic biopsy for significant prostate cancer detection. *BJU Int* 2011; 108: E171–8.
19 Lee DJ, Recabal P, Sjoberg DD, Thong A, Lee JK, *et al*. Comparative effectiveness of targeted prostate biopsy using MRI-US fusion software and visual targeting: a prospective study. *J Urol* 2016; 196: 697–702.
20 Remzi M, Fong YK, Dobrovits M, Anagnostou T, Seitz C, *et al*. The Vienna nomogram: validation of a novel biopsy strategy defining the optimal number of cores based on patient age and total prostate volume. *J Urol* 2005; 174: 1256–60.
21 Marra G, Ploussard G, Futterer J, Valerio M, EAU-YAU Prostate Cancer Working Party. Controversies in MR targeted biopsy: alone or combined, cognitive versus software-based fusion, transrectal versus transperineal approach? *World J Urol* 2019; 37: 277–87.
22 Panebianco V, Barchetti F, Sciarra A, Ciardi A, Indino EL, *et al*. Multiparametric magnetic resonance imaging vs. standard care in men being evaluated for prostate cancer: a randomized study. *Urol Oncol* 2015; 33: 17e1-7.
23 Meng X, Rosenkrantz AB, Huang R, Deng FM, Wysock JS, *et al*. The institutional learning curve of magnetic resonance imaging-ultrasound fusion targeted prostate biopsy: temporal improvements in cancer detection in 4 years. *J Urol* 2018; 200: 1022–9.
24 Mager R, Brandt MP, Borgmann H, Gust KM, Haferkamp A, *et al*. From novice to expert: analysing the learning curve for MRI-transrectal ultrasonography fusion-guided transrectal prostate biopsy. *Int Urol Nephrol* 2017; 49: 1537–44.
25 Gaziev G, Wadhwa K, Barrett T, Koo BC, Gallagher FA, *et al*. Defining the learning curve for multiparametric resonance imaging (MRI) of the prostate using MRI-transrectal ultrasonography (TRUS) fusion-guided transperineal prostate biopsies as a validation tool. *BJU Int* 2016; 117: 80–6.
26 Stabile A, Dell'Oglio P, Gandaglia G, Fossati N, Brembilla G, *et al*. Not all multiparametric magnetic resonance imaging-targeted biopsies are equal: the impact of the type of approach and operator expertise on the detection of clinically significant prostate cancer. *Eur Urol Oncol* 2018; 1: 120–8.
27 Watts KL, Frenchette L, Muller B, Ilinksy D, Kovac E, *et al*. Systematic review and meta-analysis comparing cognitive vs. image-guided fusion prostate biopsy for the detection of prostate cancer. *Urol Oncol* 2020; 38: 734.e19–734.e25.
28 Derin O, Fonseca L, Sanchez-Salas R, Roberts MJ. Infectious complications of prostate biopsy: winning battles but not war. *World J Urol* 2020; Doi: 10.1007/s00345-020-03112-3. [Epub ahead of print].

Supplementary Table 1: Results of binary logistic mixed-effects regression

Variable	*OR (95% CI)*	*P*
(Intercept)	12.5827 (2.0402–77.6005)	0.0064
X	0.8656 (0.6680–1.1217)	0.2751
Y	0.3819 (0.2254–0.6470)	0.0003
Z	1.4225 (0.9461–2.1389)	0.0903
Prostate volume	0.9710 (0.9521–0.9902)	0.0033

The Y and prostate volume odds ratios were found to be significantly different from 1, with higher values of Y and prostate volume associated with lower incidences of cancer. OR: odds ratio; CI: confidence interval

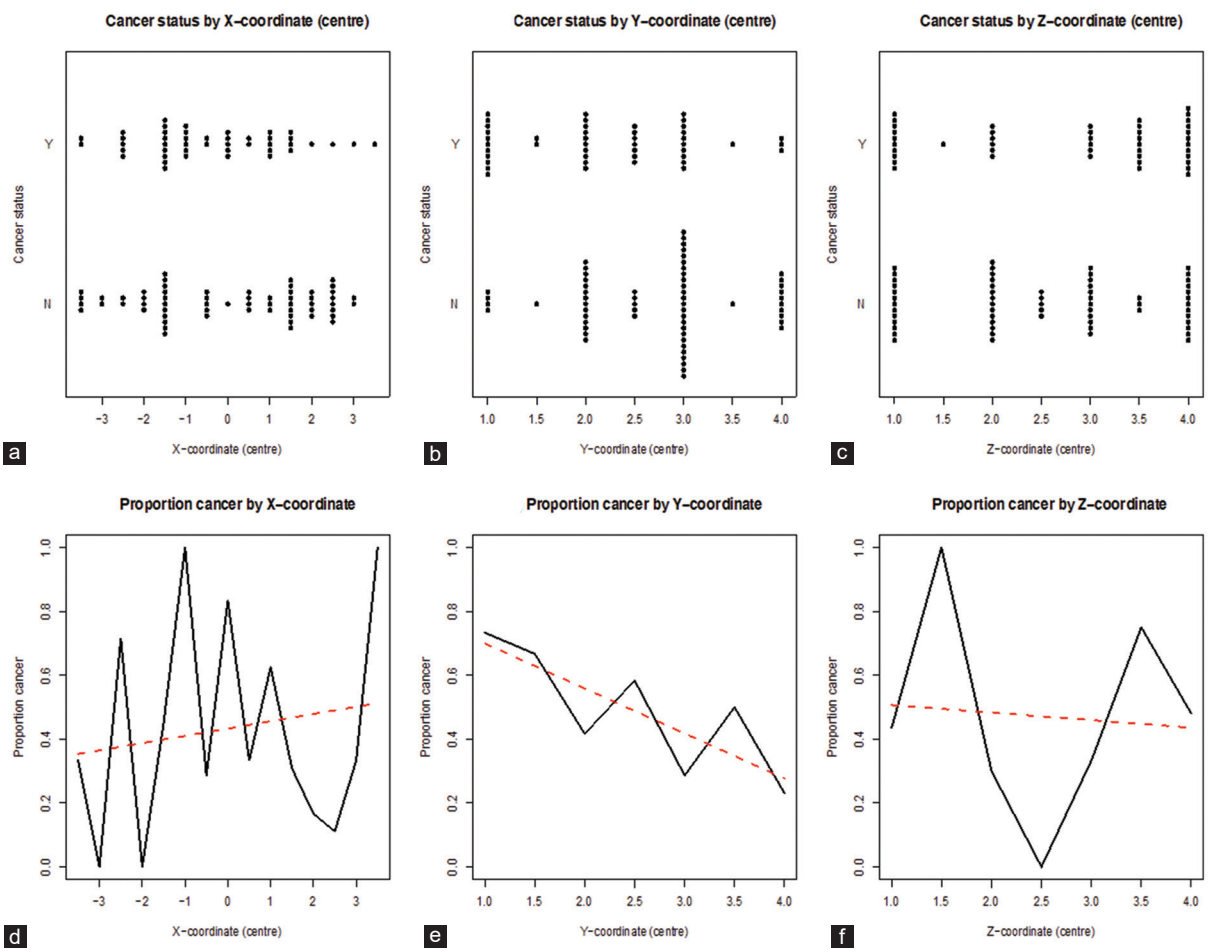

Supplementary Figure 1: One-dimensional marginal dot plots of cancer status (plots [**a-c**]) and marginals for the proportion of cancerous lesions (plots [**d-f**]) using the centroid of each lesion. In plots (**d-f**), the red-dashed line denotes the line-of-best-fit. Note, from plot (**e**), that there appears to be a possible trend along the Y-axis.